

An extended model for nonet pseudo-scalar meson fragmentation

D. Indumathi, Basudha Misra

The Institute of Mathematical Sciences, Chennai, India

Abstract : An SU(3) symmetric model with high predictivity for octet meson (π, K) quark fragmentation functions with a simple approach to SU(3) symmetry breaking (due to the relatively heavy strange quarks) is extended to the singlet sector, with some reasonable assumptions, in order to study η and η' fragmentation. Due to the presence of SU(3) symmetry, fits to the π and K data help to constrain the fragmentation functions for η and η' mesons. The use of 2-jet and 3-jet (especially the gluon jet) inclusive meson production in e^+e^- collisions and π, η inclusive production in pp collisions enable the extraction of the gluon fragmentation functions as well. While sea quarks in strange mesons (K^\pm, K^0, \bar{K}^0) and the heavier η, η' mesons are suppressed by a factor of $\lambda_H = m_\pi^2/m_H^2 \lesssim 0.1$ for $H = K, \eta, \eta'$, the gluons are not as severely suppressed: $f_g^H \sim 0.3-0.35$. A detailed parametrisation of the three independent fragmentation functions $V(x, Q^2)$, $\gamma(x, Q^2)$, and $D_g(x, Q^2)$ are given in LO QCD; *all nonet meson gluon fragmentation functions and quark fragmentation functions of all flavours* can be expressed in terms of these functions with a few model parameters including λ_H and f_g . The data prefer a nonet mixing angle $-24^\circ \leq \theta_P \leq -16^\circ$ and rule out no-mixing.

PACS Nos: 13.87.Fh, 13.65.+i, 13.60.Le, 14.40.Aq, 13.85.Ni

1 Introduction

The PHENIX experiment at RHIC [1] has measured inclusive transverse momentum spectra of η mesons in the range $p_T \approx 2-11$ GeV at mid-rapidity ($|y| \sim |\eta| < 0.35$) in pp, dAu and $AuAu$ collisions at $\sqrt{s_{NN}} = 200$ GeV. Combining with earlier data on π production [2], as well as other similar data [3], their analysis shows that the η/π^0 production ratio is roughly constant, ≈ 0.5 , for a range of center-of-mass energies ($\sqrt{s_{NN}} \approx 3-1800$ GeV). This number agrees with e^+e^- annihilation data at $\sqrt{s} = 91.2$ GeV for high scaled momentum x_p . This ratio is interesting because of its potential as a good signal for quark-gluon-plasma (QGP). Hence, a good base-line study of η fragmentation functions in pp collisions is essential for use as a normalisation factor in the study of this signal of QGP.

There are many previous studies on meson fragmentation functions at both leading order (LO) and next-to-leading order (NLO) in QCD. While the fits at NLO on π and K inclusive production presented in Ref. [4] are classic and detailed, several updated approaches have been studied [5]. While these have concentrated on the dominantly produced π and K mesons which constitute the bulk of the particle content of jets, for example, about 91% at the Z -pole, η (and η') fragmentation has not been much studied, as has been pointed out in Ref. [1]: one such study is Ref. [6].

In our earlier work [7], an SU(3) model of light quark (u, d, s) fragmentation functions for octet baryons and pseudo-scalar mesons which is in good agreement with hadro production (π and K) data in e^+e^- annihilation experiments was developed. Due to the presence of SU(3) symmetry, the model can predict the (purely octet part of the) η fragmentation functions; in fact, the pure octet η_8 fragmentation functions were listed in this paper. However, due to octet–singlet mixing, the η and η' mesons were not considered in this paper. The RHIC/PHENIX result motivates us to extend this model to the singlet sector of the pseudo-scalar mesons.

One of the main advantages of our approach is the presence of SU(3) symmetry so that the valence and sea quark fragmentation functions of the octet mesons are related to each other and can be written in terms of just three independent fragmentation functions, a valence function $V(x, Q^2)$, a sea function $\gamma(x, Q^2)$ and the gluon $D_g(x, Q^2)$. The model thus has high predictive power. SU(3) breaking effects and singlet–octet mixing are then included by introducing several parameters, which are taken to be constants in this simple-minded approach and yet give good agreement with data. In particular, it is possible to greatly improve the quality of the fits by using the abundant data on π and K inclusive production to fix the quark and gluon fragmentation functions and so to obtain both the gluon fragmentation function and quark fragmentation functions for all flavours for the η meson.

In the next section, we briefly review the cross-sections and rates for inclusive particle production in e^+e^- (2-jet and 3-jet) and pp collisions. In section 3, we highlight the salient features of the model, which is based on SU(3) flavour symmetry of the light quarks, u , d , and s . A singlet SU(3) symmetry breaking parameter, $\lambda \sim m_\pi^2/m_K^2$, incorporates the effects of strangeness suppression in the model, which has good predictivity for all the octet π and K meson fragmentation functions. The model is then extended to include the SU(3) singlet meson, along with additional parameters θ_P , f_d , f_g , that describe the singlet–octet mixing. In Section 4, the detailed phenomenology is carried out, by fitting the free parameters in comparison with known data in both the e^+e^- and pp sectors. Section 5 contains a detailed discussion and a summary of the conclusions.

2 Cross sections and rates

We consider the production of pseudo-scalar mesons in e^+e^- annihilation and pp scattering processes to leading order in perturbative QCD. We focus primarily on the production of (π , K), η and η' mesons.

2.1 e^+e^- processes

To leading order, the hadro-production cross-section in the e^+e^- scattering process at c.m. energy \sqrt{s} is [8]:

$$\frac{1}{\sigma_{tot}} \frac{d\sigma^h}{dx} = \frac{\sum_q c_q D_q^h(x, Q^2)}{\sum_q c_q} . \quad (1)$$

Here c_q are the charge factors associated with a quark q_i of flavour i and can be expressed [8] in terms of the electromagnetic charge, e_i , and the vector and axial vector electroweak couplings, $v_i = T_{3i} - 2e_i \sin^2 \theta_w$ and $a_i = T_{3i}$, as

$$\begin{aligned}
c_q &= c_q^V + c_q^A, \\
c_q^V &= \frac{4\pi\alpha^2}{s} [e_q^2 + 2e_q v_e v_q \rho_1(s) + (v_e^2 + a_e^2) v_q^2 \rho_2(s)], \\
c_q^A &= \frac{4\pi\alpha^2}{s} (v_e^2 + a_e^2) a_q^2 \rho_2(s), \\
\rho_1(s) &= \frac{1}{4 \sin^2 \theta_w \cos^2 \theta_w} \frac{s(m_Z^2 - s)}{(m_Z^2 - s)^2 + m_Z^2 \Gamma_Z^2}, \\
\rho_2(s) &= \left(\frac{1}{4 \sin^2 \theta_w \cos^2 \theta_w} \right)^2 \frac{s^2}{(m_Z^2 - s)^2 + m_Z^2 \Gamma_Z^2}.
\end{aligned} \tag{2}$$

In Eq. 1, T_3 is the third component of weak isospin, θ_w is the Weinberg angle, m_Z, Γ_Z the mass and width of the Z -boson, and a sum over quarks as well as anti-quarks is implied. Here x is the energy fraction, $x = E_{\text{hadron}}/E_{\text{beam}} = 2E_h/\sqrt{s}$. Since we neglect the hadron masses, this is the same as the momentum variable, $x_p = P_{\text{hadron}}/P_{\text{beam}} = 2P_h/\sqrt{s}$; $x^2 = x_p^2 + 4m_h^2/s$, for a hadron of mass m_h where $Q = \sqrt{s}$ is the energy scale of the interaction. The fragmentation function, $D_q^h(x, Q^2)$, is the probability at a scale Q for a quark q to hadronise to a hadron h carrying a fraction x of the energy of the fragmenting quark.

We re-express the cross section in terms of the non-singlet and singlet fragmentation function combinations, as

$$\frac{1}{\sigma^{\text{tot}}} \frac{d\sigma^h}{dx} = \frac{a_0 D_0^h(x, Q^2) + a_3 D_3(x, Q^2) + a_8 D_8(x, Q^2)}{\sum_q c_q}, \tag{3}$$

where D_0, D_3 and D_8 refer to the singlet, $D_0 = (D_u + D_d + D_s)$, and the two non-singlet combinations, $(D_u - D_d)$ and $(D_u + D_d - 2D_s)$, respectively, with $a_0 = (c_u + c_d + c_s)/3$; $a_3 = (c_u - c_d)/2$ and $a_8 = (c_u + c_d - 2c_s)/6$. Again, a sum over both quark and anti-quark flavours is implied. Note that the D_0 term dominates at the Z -pole, when $a_0 \gg a_3, a_8$.

2.2 Quark versus gluon jet fragmentation

The OPAL Collaboration [9] also has data separately on charged hadron production from quark and gluon jets. For the case of charged hadrons in quark jets, the normalised rate is given by,

$$\frac{1}{N} \frac{dN^{\text{ch}}}{dx} \Big|_q = \frac{1}{2} \sum_h \frac{1}{\sigma^{\text{tot}}} \frac{d\sigma^h}{dx}, \tag{4}$$

where $1/\sigma^{\text{tot}} d\sigma^h/dx$ is given in Eq. 3 and the sum over charged hadrons $h = \pi^+, \pi^-, K^+, K^-, K_s$ is dominated by the pionic contribution. The factor of $1/2$ occurs because the rate per quark jet is measured and there are 2 jets per process.

The more interesting data is that of charged hadrons from gluon jets. This arises in 3-jet production via $e^+e^- \rightarrow q\bar{q}g$ where the gluon jet is isolated by tagging on the (heavy) quark and anti-quark. The normalised rate here is directly proportional to the gluon fragmentation function, since the overall kinematical as well as charged factors cancel:

$$\frac{1}{N} \frac{dN^{\text{ch}}}{dx} \Big|_g = \sum_h D_g^h . \quad (5)$$

Hence the 3-jet data gives information on the gluon fragmentation function.

2.3 The pp process

In addition to the unknown fragmentation functions, hadro-production in pp processes requires information on the initial state parton density distributions. The underlying processes here are all possible qq , qg and gg ($2 \rightarrow 2$) interactions where one of the final state partons fragments into the meson of interest.

The invariant inclusive cross section for the reaction $p + p \rightarrow h + X$ for producing a hadron h at large p_T in the center of mass of the initial state protons (neglecting the transverse momentum) is given by [10],

$$E_h \frac{d^3\sigma}{dp_h^3} = \frac{1}{\pi} \sum \int_{x_a^{\min}}^1 dx_a \int_{x_b^{\min}}^1 dx_b P_a^A(x_a, Q^2) P_b^B(x_b, Q^2) \frac{d\sigma^{ab \rightarrow cd}}{z_h d\hat{t}} D_c^h(z_h, Q^2) , \quad (6)$$

where the sum over (a, b, c, d) runs over both quarks and gluons. Here x_a and x_b are the usual Bjorken- x corresponding to the parent proton momenta p_A and p_B : $x_a = p_a/p_A$, $x_b = p_b/p_B$. Hence $P_{a/A}(x_a, Q^2)$ are the usual parton density distributions; for example, $P_{u/p}(x_a, Q^2) \equiv u(x_a, Q^2)$, etc.

The fragmentation functions depend on the variables, $z = z_h = p_h/p_c$ and $Q^2 = p_T^2$ while the partonic sub-process variables are as usual defined in terms of the s , t and u hadronic variables as $\hat{s} = x_a x_b s$, $\hat{t} = x_a t/z$ and $\hat{u} = x_b u/z$. The limits of integration are [10]

$$x_a^{\min} = \frac{x_1}{1 - x_a} ; \quad x_b^{\min} = \frac{x_a x_2}{x_a - x_1} ,$$

with $x_1 = -u/s$, $x_2 = -t/s$.

For numerical comparison with the data, we reëxpress the cross-section in terms of the physical observables which are the transverse momentum $p_T = p_h \sin \theta$ and the rapidity $y = (1/2) \ln[(E_h + p_h \cos \theta)/(E_h - p_h \cos \theta)]$, as

$$E_h \frac{d^3\sigma}{dp_h^3} \equiv \frac{1}{2p_T} \frac{d^3\sigma}{dp_T dy d\phi} , \quad (7)$$

where θ is the scattering angle of the hadron h in the pp center of mass frame and E_h and p_h are its energy and 3-momentum.

The various sub-process cross-sections [11] are listed in Table 1. Note that the qq , qg and gg processes all contribute at the same order in α_s . Hence the quark and gluon fragmentation functions contribute at the same order, unlike in the e^+e^- case.

We now present details of our model for quark fragmentation functions.

Subprocess	$\frac{d\sigma^{ab \rightarrow hd}}{dt} \frac{1}{z_H}$
$q_i q_j \rightarrow q_i q_j,$ $q_i \bar{q}_j \rightarrow q_i \bar{q}_j$	$2F(\chi) + 0$
$q_i q_i \rightarrow q_i q_i$	$2F(\chi) - \frac{2}{N} \{ \chi + 2 + \frac{1}{\chi} \}$
$q_i \bar{q}_i \rightarrow q_i \bar{q}_i$ $q_i \bar{q}_i \rightarrow q_j \bar{q}_j$ $q_i \bar{q}_i \rightarrow gg$	$2F(\chi) + \{ \frac{2}{N} (\chi - 1 + \frac{1}{\chi}) + \frac{2(1+\chi^2)}{(1+\chi)^2} \}$ $0 + \{ \frac{2(1+\chi^2)}{(1+\chi)^2} \}$ $0 + \frac{N_g}{N} \{ \chi + \frac{1}{\chi} - \frac{h(1+\chi^2)}{(1+\chi)^2} \}$
$qg \rightarrow qg,$ $\bar{q}g \rightarrow \bar{q}g$	$h2F(\chi) + \{ \chi + 3 + \frac{1}{\chi} \}$
$gg \rightarrow gg$ $gg \rightarrow q\bar{q}$	$h^2 2F(\chi) + h^2 \{ 4 - \frac{2\chi}{(1+\chi)^2} \}$ $0 + \frac{N}{N_g} \{ 2(\chi + \frac{1}{\chi}) - \frac{2h(1+\chi^2)}{(1+\chi)^2} \}$

Table 1: Subprocess cross-sections in pp scattering [11] in units of $a\pi\alpha_s^2/\hat{s}^2$; $a = 4C_F^2/N_g$, $h = C_A/C_F$, with $C_F = 4/3$, $C_A = 3$, $N = 3$, and $N_g = 8$.

3 The Model

This model was developed in Ref. [7] to study π and K fragmentation in e^+e^- collisions. Consider inclusive octet hadro-production under the assumption of exact SU(3) (flavour) symmetry:

$$q_i \rightarrow h_i^j + X_j, \quad (8)$$

where $q_i = u, d, s$ for $i = 1, 2, 3$. That is, we have $3 \rightarrow 8 + X$, with X being a triplet, antisixplet or fifteenplet. This holds for both octet meson and baryon production. The fragmentation of a light quark (u, d, s) into any member of the octet is completely described by three independent fragmentation functions, $\alpha(x, Q^2)$, $\beta(x, Q^2)$, $\gamma(x, Q^2)$, corresponding to $X = 3, \bar{6}, 15$ respectively.

The corresponding fragmentation functions for the antiquarks are $\bar{\alpha}$, $\bar{\beta}$ and $\bar{\gamma}$ respectively. As the pseudo-scalar meson-octet contains both the mesons and their antiparticles, $D_q^h(x, Q^2) = D_{\bar{q}}^h(x, Q^2)$ so that there are only three independent quark fragmentation functions for the entire meson octet, which we choose to be α , β and γ .

These simplify further on applying equality of unfavoured fragmentation so that $D_u^{\pi^-} = D_d^{\pi^+} = D_s^{\pi^+} = D_s^{\pi^-}$, etc., which reduces the number of independent functions to a valence fragmentation function, $V(x, Q^2)$ and a sea fragmentation function, $S(x, Q^2)$, where

$$V = \alpha + \beta - \frac{5}{4}\gamma = \alpha - \frac{3}{4}\gamma; \quad (9)$$

$$S = 4\beta = 2\gamma. \quad (10)$$

The detailed expressions for D_q^h in terms of these functions are given in Ref. [7] and are reproduced in Table 2 in terms of V and γ .

fragmenting quark	p/K^+	fragmenting quark	n/K^0
u	: $V + 2\gamma$	u	: 2γ
d	: 2γ	d	: $V + 2\gamma$
s	: 2γ	s	: 2γ
fragmenting quark	Λ^0/η	fragmenting quark	Σ^0/π^0
u	: $\frac{1}{6}V + 2\gamma$	u	: $\frac{1}{2}V + 2\gamma$
d	: $\frac{1}{6}V + 2\gamma$	d	: $\frac{1}{2}V + 2\gamma$
s	: $\frac{4}{6}V + 2\gamma$	s	: 2γ
fragmenting quark	Σ^+/π^+	fragmenting quark	Σ^-/π^-
u	: $V + 2\gamma$	u	: 2γ
d	: 2γ	d	: $V + 2\gamma$
s	: $2\beta + \gamma$	s	: 2γ
fragmenting quark	Ξ^0/\overline{K}^0	fragmenting quark	Ξ^-/K^-
u	: 2γ	u	: 2γ
d	: 2γ	d	: 2γ
s	: $V + 2\gamma$	s	: $V + 2\gamma$

Table 2: Quark fragmentation functions into members of the baryon and meson octet in terms of the SU(3) functions $V(x)$ and $\gamma(x)$ in the exact SU(3) symmetric case.

3.1 Flavour breaking effects

Flavour SU(3) is badly broken due to the relatively heavier s -quark compared to the u - and d -quarks. This is implemented in the model through an x -independent suppression factor λ whenever a strange quark is needed in order to fragment into that meson. For example, $D_u^{K^+}$, $D_d^{K^+}$ and $D_s^{K^+}$ are suppressed by λ compared to the SU(3) symmetric expressions given in Table 2 since we require $q \rightarrow q\bar{s}$ in order to fragment into K^+ with a valence \bar{s} . While $D_u^{K^+}$ and $D_d^{K^+}$ are similarly suppressed, only the sea part of $D_s^{K^+}$ is suppressed, so that the fragmentation of \bar{s} into K^+ is given by (see Table 2),

$$D_{\bar{s}}^{K^+} = 2V + 2\lambda\gamma. \quad (11)$$

The valence component is not suppressed since the heavier strange quark is already available and only non-strange quarks are needed to produce K^+ . The sea (anti)-quark fragmentation function is suppressed since, by definition, the fragmenting (anti)-quark is in the sea of the produced hadron and a strange (anti)-quark is still needed to make up the valence quantum numbers. Similar arguments can be applied to the fragmentation functions of K^- , K^0 and \overline{K}^0 .

In short, the sea contributions to the K meson fragmentation functions remain SU(3) symmetric and are uniformly suppressed by λ compared to the corresponding unbroken SU(3) (or π) fragmentation functions. Hence, all the quark fragmentation functions, and hence the combinations D_0 , D_3 and D_8 are expressed in terms of the

octet functions, V and γ and the constant suppression factor λ , which we expect to be $\lambda \sim m_\pi^2/m_K^2$.

Until now nothing new has been introduced. We now extend this model to include the singlet mesons and SU(3) singlet–octet mixing, in order to determine the η and η' fragmentation functions.

3.2 Extension for η, η' mesons

The physical η and η' states are orthogonal admixtures of the pure SU(3) octet and singlet states, η_8 and η_1 , with mixing angle θ_P :

$$\begin{aligned}\eta &= \eta_8 \cos \theta_P - \eta_1 \sin \theta_P ; \\ \eta' &= \eta_8 \sin \theta_P + \eta_1 \cos \theta_P ,\end{aligned}$$

where $|\eta_8\rangle = (u\bar{u} + d\bar{d} - 2s\bar{s})/\sqrt{6}$ and $|\eta_1\rangle = (u\bar{u} + d\bar{d} + s\bar{s})/\sqrt{3}$. The quadratic and linear mass formulas predict θ_P to be -11.5° and -24.6° respectively; present experimental limits allow the range $-24^\circ \leq \theta_P \leq -10^\circ$ [8]. Note that θ_P is still small; $\cos \theta_P \geq 0.9$, and so η (η') is dominated by its η_8 (η_1) component.

The purely octet contributions are given in Table 2. Note that the singlet combination of the η_8 fragmentation function is given by $D_0^8 = 2V + 12\gamma$ just as for the π and K mesons. The non-singlet fragmentation functions are $D_3^8 = 0$ and $D_8^8 = -2V$.

3.3 SU(3) singlet fragmentation functions

In order to complete the description for the physical η meson, we now need to address the SU(3) singlet contributions. There is only one singlet fragmentation function that we denote as δ , since the only possibility is $3 \rightarrow 1 + X$:

$$q_i \rightarrow h + X_i , \quad (12)$$

where $q_i = u, d, s$ for $i = 1, 2, 3$, with X being a triplet alone. Instead of including an additional unknown fragmentation function, we follow a slightly different route. Since δ describes a pure SU(3) singlet fragmentation function, it should be proportional to the singlet fragmentation function D_0^8 . We set

$$\delta \equiv D_0^1 = f_d(D_0^8) = f_d(2V + 12\gamma) , \quad (13)$$

where we choose f_d to be an x -independent (unknown) constant. For the same reason, we set the non-singlet functions $D_3^1 = D_8^1 = 0$. These conditions completely determine the individual η_1 quark fragmentation functions in terms of f_d as given in Table 3.

3.4 Mass suppression effects in the η_8 fragmentation functions

3.4.1 Valence sector

We now consider SU(3) breaking effects and proceed along the lines discussed for suppression in K mesons. Since η_8 is a bound state of $q_i\bar{q}_i$ quarks of the same flavour, only the strange quark valence fragmentation functions, i.e., the valence components of D_s^8 and $D_{\bar{s}}^8$ are suppressed; this suppression is again by the same factor λ as in the kaon case.

fragmenting quark	η_1
u	$: f_d(\frac{1}{3}V + 2\gamma)$
d	$: f_d(\frac{1}{3}V + 2\gamma)$
s	$: f_d(\frac{1}{3}V + 2\gamma)$

Table 3: The unbroken SU(3) singlet η_1 fragmentation functions; f_d is a free parameter.

3.4.2 Sea sector

There is an additional complication for the sea quark fragmentation relative to the kaon sector: a sea quark has to pick up a quark–anti-quark pair of the *same* flavour so that $q_i\bar{q}_i \rightarrow \eta_8$, but all possible flavours, $i = u, d, s$, are possible because of the flavour content of the η_8 meson. If a strange quark–anti-quark pair is produced during fragmentation, the contribution is suppressed by λ , exactly as in the case of kaons.

A priori, it appears that there should be no suppression when $u\bar{u}$ or $d\bar{d}$ pairs fragment into η_8 . However, a non-strange $u\bar{u}$ or $d\bar{d}$ pair will prefer to fragment to π rather than η because of the relative masses involved. Hence, non-strange sea fragmentation to η_8 is also suppressed; since the strangeness suppression factor is $\lambda = m_\pi^2/m_K^2$, we take the non-strange suppression factor to be $\lambda_8 = m_\pi^2/m_\eta^2$. Note that we have used the relevant mass as that of the physical mass eigenstate, m_η , since the η_8 contribution dominates the η state. Since sea quark contributions to the η_8 fragmentation can arise from production of quark–anti-quark pairs of any flavour, hence they are uniformly suppressed by a factor $f_8 = (2\lambda_8 + \lambda)/3$.

3.5 Mass suppression factors in η_1 fragmentation functions

The logic is exactly the same as for the η_8 case. The valence strange sector is suppressed by λ as before while the sea sector is uniformly suppressed by a factor $f_1 = (2\lambda_1 + \lambda)/3$ where $\lambda_1 = m_\pi^2/m_{\eta'}^2$ is the non-strange suppression factor for η_1 , assuming that η_1 dominates the η' state.

3.6 The η, η' fragmentation functions

Hence, the model has been extended to include a realistic prediction of the η_8 and η_1 fragmentation functions in terms of the two octet functions V and γ and the x -independent suppression factor λ (all known from fits to π and K data), along with the x -independent suppression factors λ_8 and λ_1 apart from an unknown constant f_d .

In summary, we have, for the octet meson:

$$\begin{aligned}
D_u^8 = D_d^8 &= \frac{1}{6}V + 2f_8\gamma, \\
D_s^8 &= \frac{2}{3}V\lambda + 2f_8\gamma,
\end{aligned}$$

and for the singlet meson:

$$D_u^1 = D_d^1 = f_d \left(\frac{1}{6}V + 2f_1\gamma \right) ,$$

$$D_s^1 = f_d \left(\frac{2}{3}V\lambda + 2f_1\gamma \right) .$$

The fragmentation functions for the physical states can then be expressed in terms of the fragmentation functions for the η_8 and η_1 parts, along with the mixing angle, θ_P . We have

$$D_i^\eta = (c_i^\eta)^2 \left(\cos^2 \theta_P \frac{D_i^8}{(c_i^8)^2} + \sin^2 \theta_P \frac{D_i^1}{(c_i^1)^2} \right) , \quad (14)$$

$$D_i^{\eta'} = (c_i^{\eta'})^2 \left(\sin^2 \theta_P \frac{D_i^8}{(c_i^8)^2} + \cos^2 \theta_P \frac{D_i^1}{(c_i^1)^2} \right) , \quad (15)$$

where $i = u, d, s$ and the coefficients are $c_u^8 = c_d^8 = 1$, $c_s^8 = -2$, $c_u^1 = c_d^1 = c_s^1 = \sqrt{2}$, $c_u^\eta = c_d^\eta = (\cos \theta_P - \sqrt{2} \sin \theta_P)$, and $c_s^\eta = (-2 \cos \theta_P - \sqrt{2} \sin \theta_P)$. The coefficients for η' are obtained from those of η by the substitution: $(\cos \theta_P \rightarrow \sin \theta_P; \sin \theta_P \rightarrow -\cos \theta_P)$.

4 Comparison with the data

We now fit the unknown model parameters by a comparison with data. Note that the octet fragmentation functions $V(x, Q^2)$ and $\gamma(x, Q^2)$, the suppression factor, λ , and the gluon fragmentation function $D_g(x, Q^2)$, have already been fitted to the π and K data in Ref. [7]. We consider them here again for reasons explained below.

4.1 $e^+e^- \rightarrow 2$ -jets

The V and γ were fitted to parametrised forms as a function of x :

$$F_i(x) = a_i(1-x)^{b_i}(x^{c_i})(1+d_i x + e_i x^2) , \quad (16)$$

at a starting scale of $Q_0^2 = 2 \text{ GeV}^2$ and evolved, along with the gluon fragmentation function, $D_g(x, Q^2)$, to leading order (LO) in perturbative QCD. Best fits to $V(x, Q_0^2)$, $S(x, Q_0^2)$, $D_g(x, Q_0^2)$ and λ were obtained from fits to electro-production data at the Z -pole $Q^2 = 91.2^2 \text{ GeV}^2$ for π^\pm and K^\pm [12].

The best-fit values for the parameters a, b, c, d, e for different input fragmentation functions are given in Table 4. The best fit value for λ is

$$\lambda = 0.08 , \quad (17)$$

which is consistent with the quark model expectation $\lambda = m_\pi^2/m_K^2$.

The resulting fits to the π and K production rates at the Z -pole from LEP data [13, 14] are shown in Fig. 1. Note that the gluon is not well-determined from this data, unlike the quark fragmentation functions. This is because the cross-sections are functions only of the quark fragmentation functions at LO and the gluon contribution only enters through the evolution equations. The electro-production rates are insensitive to the gluon even at next-to-leading order (NLO) since the gluon contribution

is down by a factor of α_s compared to the quark contributions. Three-jet processes are sensitive to the gluon contribution; we return to this point later.

Note that the sea quark and gluon distributions are different from those obtained in Ref. [7]. Since gluons and sea quarks mix during singlet evolution, a small non-zero gluon was included earlier while evolving from the starting scale $Q_0^2 = 2 \text{ GeV}^2$ to the observed scale Q^2 . Gluon fragmentation function data is now available [9] from isolating charged hadrons produced from gluon jet fragmentation in $e^+ e^- \rightarrow q\bar{q}g$ processes. It turns out that the gluon fragmentation used in Ref. [7] is too small and therefore incompatible with the 3-jet data. Our new updated fits here include a gluon that is consistent with such data (as discussed below); this necessitates a revision of the sea quark *starting* fragmentation functions (they have been made smaller) so that the sea contribution evolved to the Z -pole (with the contribution from the new enhanced gluon) still matches the earlier result (and hence the data).

The valence function $V(x, Q_0^2)$ remains the same as before.

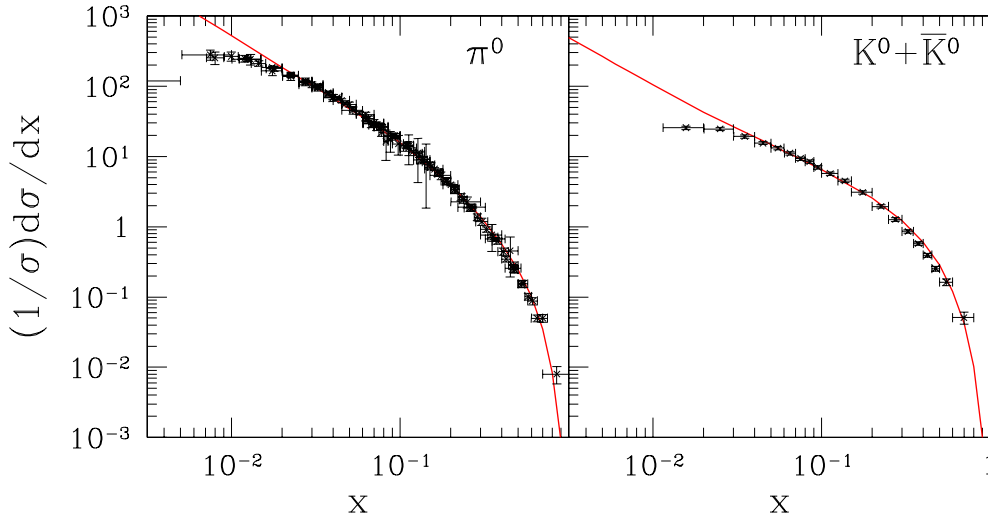


Figure 1: The model fits to the Z -pole data for π^0 [13] and $K^0 + \bar{K}^0$ [14] mesons; the functions at the starting scale $Q_0^2 = 2 \text{ GeV}^2$ are given in Table 4.

It is observed that the predictions exceed the data systematically at small- x . This is because of the pole in the P_{qq} and P_{gg} splitting functions as $x \rightarrow 0$ which cause the DGLAP evolution to drive the small- x sea and gluon fragmentation functions to large values which cause the DGLAP evolution to drive the small- x sea and gluon fragmentation functions to large values. While the starting values of the fragmentation functions are integrable, this evolution makes them non-integrable due to this increase at small- x . However, the fragmentation functions should remain integrable (as their first moments are related to the hadron multiplicities). An approach such as the modified leading log approximation (MLLA) [15] cures the small- x divergence and gives a good fit to the data at small- x as has been discussed in Ref. [7]; here we simply ignore the small- x region and concentrate on the fits for $x \gtrsim 0.02$ for all mesons under consideration.

	$2V$	2γ	$2g$
a	2.33	3.5	7.25
b	2.15	12.76	4.4
c	-0.64	-0.75	-0.5
d	5.35	3.87	2
e	-5.12	61.59	0

Table 4: Input values at $Q^2 = 2 \text{ GeV}^2$ for the valence, sea and gluon fragmentation functions for the pseudo-scalar meson octet. The factor of 2 is due to the convention used in the earlier work [7] when the model was fitted to the *sum* of the charged hadrons, for example, $\pi^+ + \pi^-$, $K^+ + K^-$, etc.

4.1.1 Fits to η , η' data on the Z pole

With λ_8 and λ_1 fixed to the theoretically expected values, f_d is the only unknown parameter in the rates for both η and η' production. Since the nonet mixing angle θ_P is small, f_d is mostly constrained by the large- x data. Fits to the η , η' production rates in e^+e^- annihilation on the Z -pole at LEP [16, 17] yield a best fit value to the free parameter of $f_d = 0.3$. However, the electro-production data are insensitive to the nonet mixing angle θ_P , as can be seen from the fits to the data in Fig. 2 where the fits for $\theta_P = 0^\circ$, -15° and -24° are shown. The allowed range of θ_P marginally alters the fits at small- x values, while being completely insensitive in the large- x region.

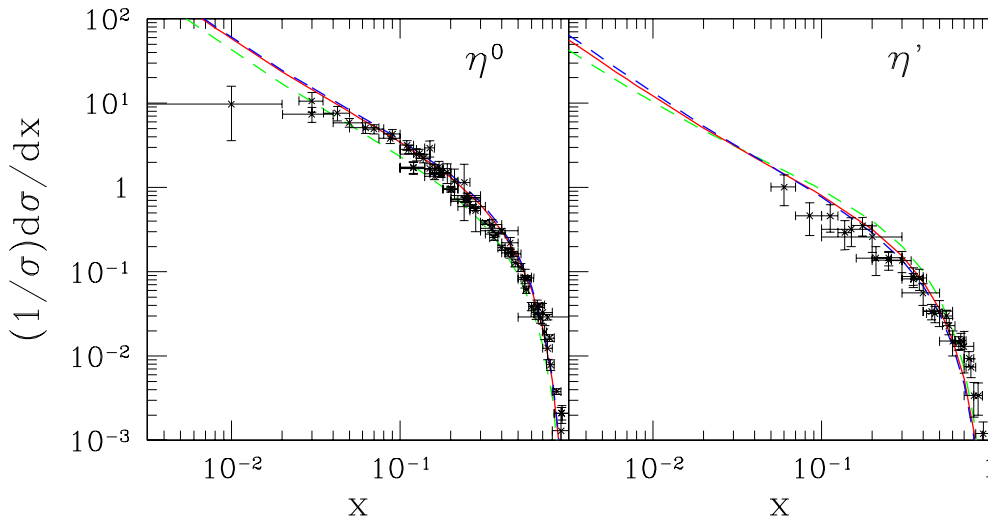


Figure 2: The figure shows the model fits at $\sqrt{s} = 91.2 \text{ GeV}$ to the LEP data on η [16] and η' [17] mesons as a function of x with both x and y error-bars. The green, red and blue lines represent $\theta_P = 0^\circ$, -15° and -24° respectively for $f_d = 0.3$.

4.2 $pp \rightarrow (\pi, \eta)X$

The PHENIX experiment at RHIC [2, 1] has measured the inclusive transverse momentum spectra of π and η mesons in the range $p_T \approx 1.5\text{--}14 \text{ GeV}/c$ at mid-rapidity ($|\eta| < 0.35$) in pp , dAu and $AuAu$ collisions at $\sqrt{s_{NN}} = 200 \text{ GeV}$. They have also

measured the η/π^0 production ratio, R_{η/π^0} . This ratio is interesting because of its potential as a good signal for quark-gluon-plasma.

The η/π^0 ratio in pp collisions is the base-line with which comparisons in dA or AA processes are made. It is therefore important to understand and correctly determine this ratio in pp collisions for a wide range of Q^2 ($\sim p_T^2$). As can be seen from Eq. 6, this depends on the initial parton density distributions and the final state fragmentation functions. Furthermore, the gluon and quark fragmentation functions (and density distribution functions) occur at the same order in α_s . The study of such a process, therefore, may help determine the gluon fragmentation functions with much greater accuracy than currently known. With these two considerations in view, the model was compared to the η and π production rates in pp collisions.

4.2.1 Analytical approximation

Before comparing the model to the data, it is observed that there is considerable simplification of the expressions when the pp sub-process cross-sections are reexpressed as a constant times a kinematic factor, $F(\chi)$, with small correction terms [11], as can be seen from Table 1, where

$$F(\chi) = \chi^2 + \chi + 1 + \frac{1}{\chi} + \frac{1}{\chi^2}, \quad (18)$$

where $\chi = \hat{u}/\hat{t}$. When these correction terms are dropped, the surviving terms are such that the fragmenting parton c has the same flavour as the initial parton a . Then, apart from an overall factor,

$$f = \frac{C_F^2}{N_g} \frac{4\pi\alpha_s^2}{\hat{s}^2}, \quad (19)$$

the integrand of Eq. 6 for the hadro-production rate can be factorised as the product of two terms:

$$\sum_{i,j} \left(q_i D_i^h + \bar{q}_i \bar{D}_i^h + h g D_g^h \right) \times (q_j + \bar{q}_j + h g) . \quad (20)$$

The first term depends on (x_a, z) and contains the dependence on the unknown fragmentation functions while the second term depends on x_b alone. In this factorised form it is clear that there is a substantial dependence on the gluon fragmentation function only when the corresponding gluon density distribution function is large as well; this occurs, for the central rapidity region measured by PHENIX at RHIC, for low p_T , $p_T \lesssim 5$ GeV. Hence, the small- p_T data (with $Q^2 \approx p_T^2 \geq 2$ GeV²) should be sensitive to the gluon fragmentation function. Since our input fragmentation functions are at a scale $Q_0^2 = 2$ GeV², there may be significant threshold effects at this energy; we choose $Q^2 = (p_T^2 + m_h^2)$ with $Q^2 > Q_0^2$.

4.3 Fits to the π production rate

The expressions for the production rate are integrated over the central rapidity region, $-0.35 \leq y \leq 0.35$, and over the allowed ranges of x_a and x_b for a given p_T . The fits to the π production data [2] as a function of p_T are shown in Fig. 3. Here the exact expressions for the sub-process cross-sections have been used, not the approximations discussed in the previous sub-section. The small- p_T data, as expected (where $z_h \gtrsim$

0.02), are very sensitive to the gluon fragmentation function, while the larger p_T data ($z_h \gtrsim 0.1$) are sensitive to the quark fragmentation functions. The effect of scale, $Q^2 = f_S(p_T^2 + m_h^2)$, $f_S = 0.5-2$, is also shown in the figure.

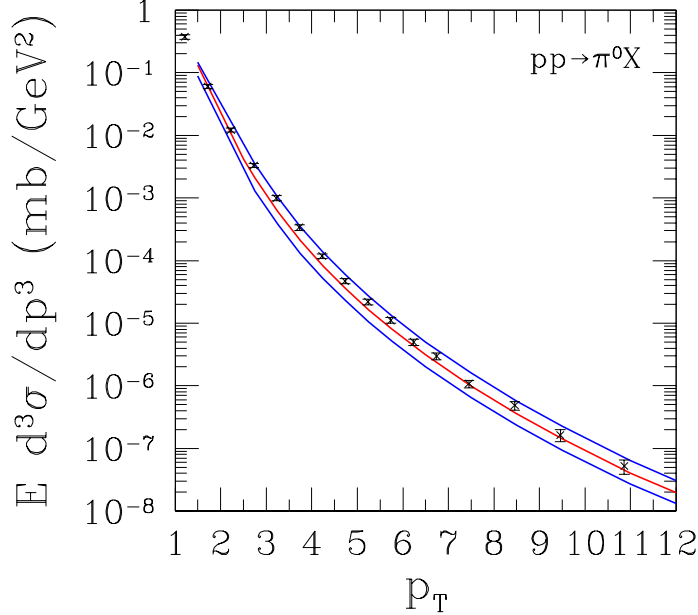


Figure 3: The π production rate in pp collisions at $\sqrt{s} = 200$ GeV in comparison with the RHIC/PHENIX data [2]. The central curve corresponds to $Q^2 = p_T^2 + m_h^2$ while the upper (lower) curve corresponds to a value of Q^2 half (twice) this value.

4.4 Fits to the η production rate

It is reasonable to assume that the gluon fragmentation function in η is suppressed relative to that of π , just as is the case with sea quarks. However, there is a difference during evolution: the gluon mixes with the entire singlet combination, D_0^η , which contains both valence and sea quark terms. For example,

$$\begin{aligned} D_0^\pi &= 2V + 12\gamma ; \\ D_0^K &= \frac{(1+\lambda)}{2} 2V + \lambda 12\gamma ; \\ D_0^\eta &= x_0 2V + y_0 12\gamma ; \end{aligned}$$

where

$$\begin{aligned} x_0 &= \frac{1}{6} [2(c_u^\eta)^2 + \lambda(c_s^\eta)^2] (\cos^2 \theta_P + \sin^2 \theta_P) , \\ \theta_P \xrightarrow{\text{small}} &\sim 0.5 ; \\ y_0 &= \frac{f_8}{12} (\cos^2 \theta_P [8(c_u^\eta)^2 + (c_s^\eta)^2] + f_d f_1 \sin^2 \theta_P [4(c_u^\eta)^2 + 2(c_s^\eta)^2]) , \\ \theta_P \xrightarrow{\text{small}} &f_8 . \end{aligned} \tag{21}$$

Hence the valence in $D_0^{K,\eta}$ is suppressed by a factor of 1/2 and the sea is suppressed by λ, f_8 compared to D_0^π . Therefore, we expect the gluon fragmentation into η to be suppressed by $D_g^\eta \sim D_g^K = f_g D_g^\pi$, where $y_0 \leq f_g \leq x_0$.

Since V and γ dominate in different regions of phase-space (at different z_h values), it is likely that f_g is an x -dependent suppression factor. This can be studied in 3-jet processes in e^+e^- collisions (see the next sub-section). Since detailed data on this is still not available, we assume f_g to be an x -independent constant between y_0 and x_0 ; certainly $f_g \leq 1$.

The resulting fits to the η production rate in pp collisions are shown in Fig. 4 for different allowed mixing angles θ_P . While the data is sensitive to f_g , as expected, it does not appear to be very sensitive to θ_P . Note that the maximum separation between the curves for a given mixing angle is at small- p_T , where the gluon contributes maximally. At large enough p_T , the ratio should determine θ_P as the gluon contribution becomes negligible.

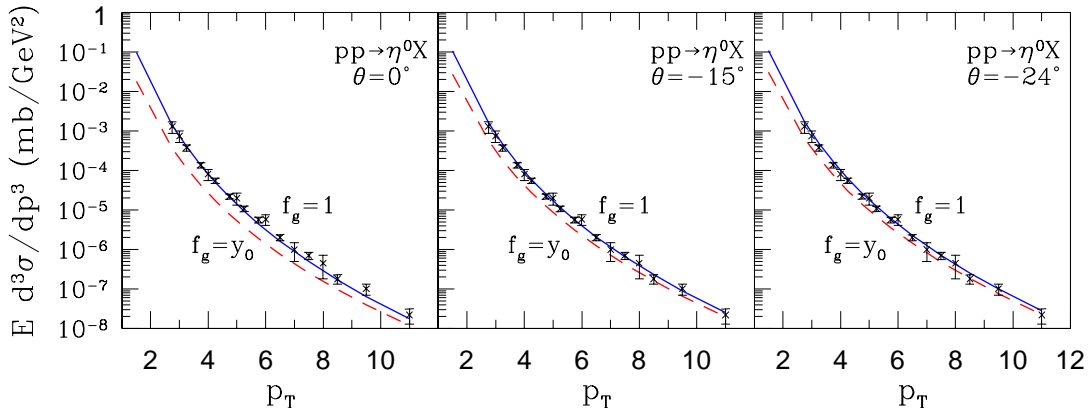


Figure 4: The η production rate in pp collisions at $\sqrt{s} = 200$ GeV as a function of p_T with $Q^2 = p_T^2 + m_h^2$ in comparison with the RHIC/PHENIX data [1].

4.5 Fits to the η/π^0 ratio

The sensitivity to both f_g and θ_P is amplified in the η/π ratio, as can be seen in Fig. 5 where the RHIC/PHENIX data [1] are also superposed. The region bounded by the curves for $f_g = y_0, 1$ in the figure encompass the possible fits to the ratio.

A χ^2 minimisation gives a best fit for $f_g = 0.3, \theta_P = -20.0^\circ$. Since the total errors are large, only the statistical errors were used in the fit to give $\chi^2 = 9.5$ for 11 d.o.f. A fit with the total errors reduces this best fit value to $\chi^2 = 4.5$. The saturation value of the η/π ratio increases with increasing $|\theta_P|$. Constraining the large p_T ratio to be ~ 0.5 [1] as favoured by PYTHIA [18] decreases the value of θ_P to about -16° ; however, the errors on the data also allow this ratio to saturate at values of around 0.6. An improvement in the data quality will definitely constrain both θ_P and f_g better. Currently, a reasonable quality of fit ($\chi^2 \sim$ d.o.f.) is obtained in a range $f_g = 0.3\text{--}0.35$ and $-24^\circ \leq \theta_P \leq -16^\circ$. Also, while the π and η production rates are scale dependent, this dependence is very small and virtually cancels out in the ratio, except for a mild dependence at smaller p_T values, $p_T \lesssim 3$ GeV.

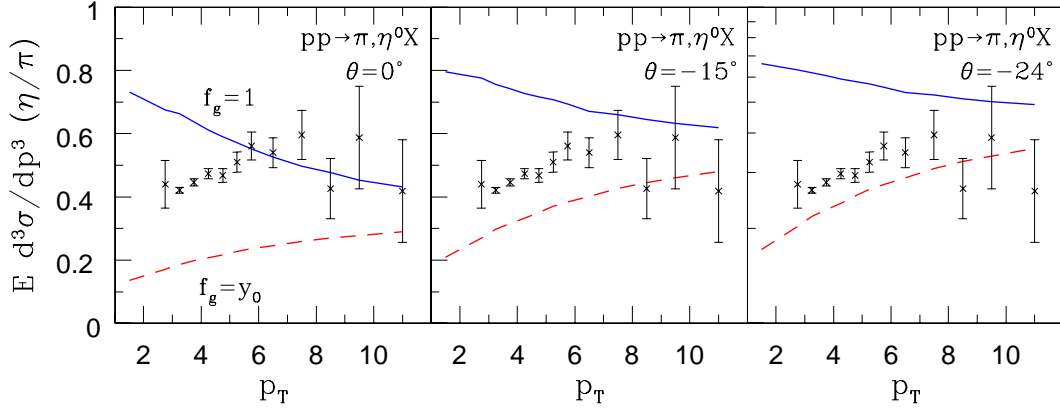


Figure 5: The η/π production ratios in pp collisions as a function of p_T for different nonet mixing angle θ_P for two different gluon suppression factors, $f_g = y_0, 1$, in comparison with the RHIC/PHENIX data at $\sqrt{s} = 200$ GeV [1]

The quality of fits to the η/π ratio for the typical choices: $(f_g, \theta_P) = (0.3, -20^\circ)$ and $(0.35, -16.77^\circ)$, are shown in Fig. 6 along with the RHIC/PHENIX data where both statistical and total errors are shown.

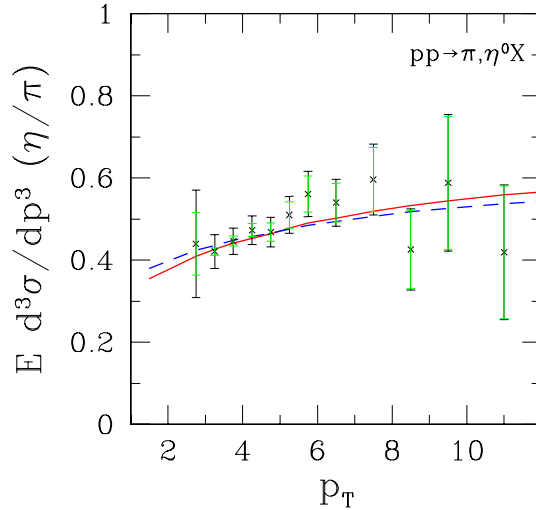


Figure 6: The η/π production ratios in pp collisions as a function of p_T for $(f_g, \theta) = (0.3, -20^\circ)$ (solid line) and $(0.35, -16.77^\circ)$ (dashed line) in comparison with the RHIC/PHENIX data [1] at $\sqrt{s} = 200$ GeV.

4.6 Fits to the 3-jet data in e^+e^- collisions

Fits to the individual quark fragmentation functions are of the same quality as for the π, K production discussed earlier (this data is just the sum of the π and K rates). Hence we do not discuss them further and proceed directly to gluon jet fragmentation.

With $f_g = 0.3$ as determined from fits to the η/π ratio in pp collisions, it is now possible to compute the charged hadron production rate from gluon fragmentation in $e^+ e^- \rightarrow q\bar{q}g$. We have, from Eq. 5,

$$\begin{aligned} \left. \frac{1}{N} \frac{dN^{\text{ch}}}{dx} \right|_g &= \sum_h D_g^h \\ &= 2.9\text{--}3.2 D_g^\pi, \end{aligned}$$

where we have assumed that $f_g^K = f_g^\eta = 0.3\text{--}0.35$, so that the gluon fragmentation into η and K are roughly suppressed by the same factor. If π and K production from gluon jets is separately measured, f_g (and its x -dependence, if any) can be easily determined. Such data would be very useful in constraining further the small- p_T behaviour of the η/π ratio.

The resulting fit to the OPAL data [9] is shown in Fig. 7. Notice that the Q^2 scales of the $e^+ e^-$ and pp processes are very different: the former with a value $Q^2 \sim 80^2 \text{ GeV}^2$ (slightly smaller than the Z -pole value for 2-jet production), and the latter with $Q^2 = p_T^2 = 2^2\text{--}14^2 \text{ GeV}^2$. Due to the pole in the P_{gg} splitting function, the gluon fragmentation function is very different (in fact, at both large and small z_h values) in the two cases and gives a strong consistency check on the fits to the gluon fragmentation function.

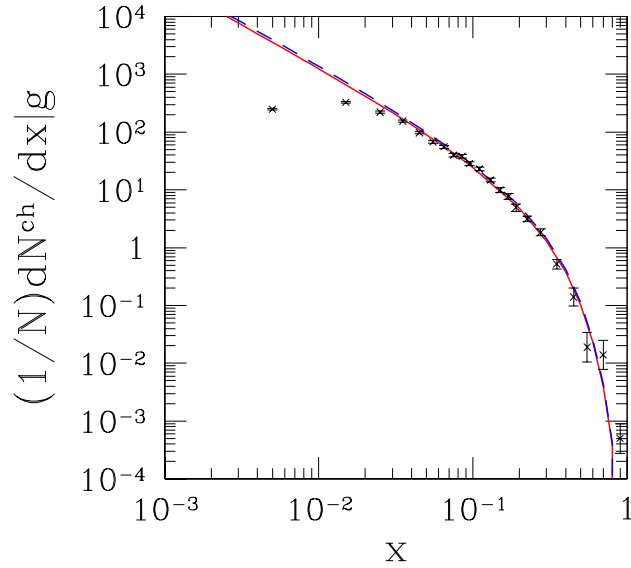


Figure 7: The normalised charged hadron production rate from gluon jets in $e^+ e^- \rightarrow q\bar{q}g$ at a mean $Q^2 = 80^2 \text{ GeV}^2$ at LEP/OPAL [9] along with the theoretical prediction $\sum_h D_g^h \sim 2.9\text{--}3.2 D_g^\pi$ where h runs over all charged hadrons and K_S . The lower (upper) curve corresponds to the choice of 2.9 (3.2), although the separation between them is not well-marked.

5 Discussion and Conclusions

Quark and gluon fragmentation functions of π , K , η , and η' mesons have been determined through a study of hadro-production rates in both e^+e^- and pp collisions. Detailed information on the η fragmentation functions has become important since the variation of the η/π production ratios in pp , pA and AA collisions is a possible signal of quark gluon plasma (QGP).

All calculations have been performed at leading order (LO) in QCD. Inclusion of NLO terms should not affect the quality of the fits, especially that of the gluons, since they have been mostly determined from ratios (normalised charged hadro-production in $e^+e^- \rightarrow 3$ -jets and η/π production ratio in pp collisions). Of course, numerical details, such as the fits to the quark and gluon fragmentation functions at the starting scale $Q_0^2 = 2 \text{ GeV}^2$, will change. The fits therefore are mainly driven, and limited by, *the model assumptions*.

A simple SU(3) model for octet meson production (π, K), has been extended to include η and η' production. Due to SU(3) symmetry, the quark fragmentation functions of all mesons are related to a common valence $V(x, Q^2)$ and sea quark $\gamma(x, Q^2)$ fragmentation function. SU(3) breaking due to the heavier strange quark is included through a constant parameter λ . Inclusion of singlet–octet mixing causes SU(3) breaking in the sea sector as well; this is parametrised by a nonet mixing angle θ_P that is known to be small ($-24^\circ \leq \theta_P \leq -10^\circ$), and a few additional constants, λ_8 , λ_1 , and f_d .

While λ , λ_8 and λ_1 are fixed from model considerations, the data, especially on the K/π ratio in e^+e^- collisions, also yields the same value of λ as that predicted by the model. The parameter f_d that occurs in the singlet fragmentation functions is fitted from η and η' data in e^+e^- collisions on the Z -pole.

Finally, suppression of gluon fragmentation in K, η relative to π is parametrised by $f_g(x)$. In the absence of more detailed data (for instance, on individual π, K production from gluon fragmentation in 3-jet processes at LEP), f_g is taken to be constant and fitted from the large- p_T ($2 \leq p_T \leq 11 \text{ GeV}$) η/π ratio in pp collisions at $\sqrt{s} = 200 \text{ GeV}$.

This gluon parametrisation, with $f_g \sim 0.3\text{--}0.35$, is completely consistent with 3-jet data in e^+e^- collisions at a very different scale $Q^2 \sim 80^2 \text{ GeV}^2$, where the gluon fragmentation is explicitly studied.

A comprehensive set of gluon and quark fragmentation functions (for all flavours) is therefore available for the set of nonet pseudo-scalar mesons, $\pi^{\pm,0}$, K^\pm , K^0 , \bar{K}^0 , η , and η' , starting with a simple model with reasonable assumptions, that is consistent with hadro-production data in both e^+e^- and pp collisions. The focus of this paper was the extension of the earlier fits [7] in π and K to the case of η and η' mesons.

Acknowledgement : We thank H.S. Mani and M.V.N. Murthy for many detailed discussions.

References

- [1] S.S. Adler et al., PHENIX Collab., Phys. Rev. **C 75**, 024909 (2007); arXiv:nucl-ex/0611006;
data from http://www.phenix.bnl.gov/WWW/talk/pub_papers.php
- [2] S.S. Adler et al., PHENIX Collab., Phys. Rev. Lett. **91**, 241803 (2003); arXiv:hep-ex/0304038;
data from http://www.phenix.bnl.gov/WWW/talk/pub_papers.php
- [3] S.S. Adler et al., PHENIX Collaboration, Phys.Rev. **C 75**, 024909 (2007);
C. Kourkouvelis et al., AFS Collaboration, Phys. Lett. **B 84**, 271 (1979) and Phys. Lett. **B 84**, 277 (1979);
T. Akesson et al., AFS Collaboration, Phys. Lett. **B 178**, 447 (1986);
T. Akesson et al., AFS Collaboration, Z. Phys. **C 18**, 5 (1983)
- [4] B.A. Kniehl, G. Kramer, B. Pötter, Nucl. Phys. **B 582**, 514-536 (2000)
- [5] S. Albino, arXiv:0810.4255, (2008);
E. Christova, E. Leader, arXiv:0809.0191, (2008);
F. Arleo, D. d'Enterria, Phys. Rev. **D 78**, 094004 (2008), arXiv:0807.1252v2;
S. Kretzer, Phys. Rev. **D 62**, 054001 (2000), arXiv:hep-ph/0003177;
D. de Florian, R. Sassot, M. Stratmann, Phys. Rev. **D76**, 074033 (2007), arXiv:0707.1506v1 [hep-ph] and Phys. Rev. **D75**, 114010 (2007), arXiv:hep-ph/0703242;
M. Hirai, S. Kumano, T.-H. Nagai, K. Sudoh, arXiv:0705.2791v1 [hep-ph], in proceedings of 42nd Rencontres de Moriond on QCD and high energy hadronic interactions, La Thuile, Italy, 17-24 Mar 2007;
S. Albino, B.A. Kniehl, G. Kramer, Nucl. Phys. **B 734**, 50-61 (2006), arXiv:hep-ph/0510173;
S. Kretzer, Acta Phys. Polon. **B 36**. 179 (2005), arXiv:hep-ph/0410219
- [6] M. Greco, S. Rolli, A. Vicini, Z. Phys. **C 65**, 277-284 (1995), arXiv:hep-ph/9404228;
M.Greco, S.Rolli, Z. Phys. **C 60**, 169-174 (1993), arXiv:hep-ph/9304311
- [7] D. Indumathi, Anubha Rastogi, H.S. Mani, Phys. Rev. **D**, 094014 (1998); arXiv:hep-ph/9802324
- [8] The Review of Particle Physics, Particle Data Group, C. Amsler et al., Phys. Lett. **B 667**, 1 (2008)
- [9] The OPAL Collaboration, G. Abbiendi et al., Eur. Phys. J. **C 11**, 217-238, 1999; arXiv:hep-ex/9903027
- [10] J.F. Owens, E. Reya, M. Glück, Phys. Rev. **D 18**, 1501 (1978);
J.F. Owens and J. D. Kimel, Phys. Rev. **D 18**, 3313, (1978);
S.M. Beran, J.D. Bjorken, and J. B. Kogut, Phys. Rev. **D 4**, 3388, (1971)
- [11] B.L. Combridge and C.J. Maxwell, Nucl. Phys. **B 239**, 429 (1984)

- [12] For a review and comprehensive compilation of (older) data in e^+e^- processes, see G.D. Lafferty, P.I. Reeves, M. R. Whalley, J. Nucl. Part. Phys. G 21, A1–A151, (1995); the individual π , K , η and η' Z -pole data used in the fits are separately listed.
- [13] Adeva et al., L3 Collaboration, Phys. Lett. **259B**, 199 (1991);
 Acciarri et al., L3 Collaboration, Phys. Lett. **328B**, 223 (1994);
 Acciarri et al., L3 Collaboration, Phys. Lett. **328B**, 223 (1994);
 Adam et al., DELPHI Collaboration, Zeit. Phys. **C69**, 561 (1995);
 Barate et al., ALEPH Collaboration, Zeit. Phys. **C74**,451 (1997);
 Ackerstaff et al., OPAL Collaboration, Eur. Phys. J. **C5**, 411 (1998);
 Barate et al., ALEPH Collaboration, Phys. Rep. **294**,1 (1998);
 Barate et al., ALEPH Collaboration, Eur. Phys. J. **C16**,613 (2000);
 Abbiendi et al., OPAL Collaboration, Eur. Phys. J. **C17**, 373 (2000)
- [14] Buskulic et al., ALEPH Collaboration, Zeit. Phys. **C64**, 361 (1994);
 Abreu et al., DELPHI Collaboration, Zeit. Phys. **C65**, 587 (1995);
 Akers et al., OPAL Collaboration, Zeit. Phys. **C67**, 389 (1995);
 Barate et al., ALEPH Collaboration, Phys. Rep. **294**, 1 (1996);
 Abe et al., SLD Collaboration, Phys. Rev. **D59**, 052001 (1999);
 Barate et al., ALEPH Collaboration, Eur. Phys. J. **C16**, 613 (2000);
 Abbiendi et al., OPAL Collaboration, Eur. Phys. **C17**, 373 (2000)
- [15] Yu.L. Dokshitzer, V.A. Khoze, A.H. Mueller and S.I. Troyan, Rev. Mod. Phys. **60**, 373 (1988);
 Yu.L. Dokshitzer, V.A. Khoze, A.H. Mueller and S.I. Troyan, Basics Of Perturbative QCD (Editions Frontieres) 1991.
- [16] Adriani et al., L3 Collaboration, Phys. Lett. **286B**, 403 (1992);
 Buskulic et al., ALEPH Collaboration, Phys. Lett. **292B**, 210 (1992);
 Acciarri et al., L3 Collaboration, Phys. Lett. **328B**, 223 (1994);
 Barate et al., ALEPH Collaboration, Phys. Rep. **294**, 1 (1996);
 Ackerstaff et al., OPAL Collaboration, Eur. Phys. J. **C5**, 411 (1998);
 Barate et al., ALEPH Collaboration, Eur. Phys. J. **C16**, 613 (2000);
 Abbiendi et al., OPAL Collaboration, Eur. Phys. J. **C17**, 373 (2000);
 Heister et al., ALEPH Collaboration, Phys. Lett. **B528**, 19 (2002)
- [17] Buskulic et al., ALEPH Collaboration, Phys. Lett. **292B**, 210 (1992);
 Barate et al., ALEPH Collaboration, Phys. Rep. **294**, 1 (1996);
 Acciarri et al., L3 Collaboration, Phys. Lett. **B393**, 465 (1997);
 Ackerstaff et al., OPAL Collaboration, Eur. Phys. J. **C5**, 411 (1998);
 Barate et al., ALEPH Collaboration, Eur. Phys. J. **C16**, 613 (2000)
- [18] For a detailed comparison to the RHIC/PHENIX data, see Ref. [1]. For details on the PYTHIA computation, see T. Sjöstrand et al., Comput. Phys. Comm. **135**, 238 (2001)